NeuroImage 87 (2014) 323–331

Contents lists available at ScienceDirect

NeuroImage

journal homepage: www.elsevier.com/locate/ynimg

Direct, intraoperative observation of ~0.1 Hz hemodynamic oscillations in awake human cortex: Implications for fMRI

Aleksandr Rayshubskiy [a], Teresa J. Wojtasiewicz [c], Charles B. Mikell [c], Matthew B. Bouchard [a], Dmitriy Timerman [a], Brett E. Youngerman [c], Robert A. McGovern [c], Marc L. Otten [c], Peter Canoll [d], Guy M. McKhann II [c], Elizabeth M.C. Hillman [a,b,*]

[a] Laboratory for Functional Optical Imaging, Department of Biomedical Engineering, Columbia University, USA
[b] Department of Radiology, Columbia University, USA
[c] Department of Neurosurgery, Columbia University, USA
[d] Department of Pathology and Cell Biology, Columbia University, USA

ARTICLE INFO

Article history:
Accepted 21 October 2013
Available online 1 November 2013

Keywords:
0.1 Hz oscillation
Resting state
fMRI
Intraoperative optical imaging
Vasomotion
Cerebral hemodynamics

ABSTRACT

An almost sinusoidal, large amplitude ~0.1 Hz oscillation in cortical hemodynamics has been repeatedly observed in species ranging from mice to humans. However, the occurrence of 'slow sinusoidal hemodynamic oscillations' (SSHOs) in human functional magnetic resonance imaging (fMRI) studies is rarely noted or considered. As a result, little investigation into the cause of SSHOs has been undertaken, and their potential to confound fMRI analysis, as well as their possible value as a functional biomarker has been largely overlooked.

Here, we report direct observation of large-amplitude, sinusoidal ~0.1 Hz hemodynamic oscillations in the cortex of an awake human undergoing surgical resection of a brain tumor. Intraoperative multispectral optical intrinsic signal imaging (MS-OISI) revealed that SSHOs were spatially localized to distinct regions of the cortex, exhibited wave-like propagation, and involved oscillations in the diameter of specific pial arterioles, indicating that the effect was not the result of systemic blood pressure oscillations. fMRI data collected from the same subject 4 days prior to surgery demonstrates that ~0.1 Hz oscillations in the BOLD signal can be detected around the same region. Intraoperative optical imaging data from a patient undergoing epilepsy surgery, in whom sinusoidal oscillations were not observed, is shown for comparison.

This direct observation of the '0.1 Hz wave' in the awake human brain, using both intraoperative imaging and pre-operative fMRI, confirms that SSHOs occur in the human brain, and can be detected by fMRI. We discuss the possible physiological basis of this oscillation and its potential link to brain pathologies, highlighting its relevance to resting-state fMRI and its potential as a novel target for functional diagnosis and delineation of neurological disease.

Introduction

It is well known that the brain exhibits baseline variations in blood flow with temporal frequencies between ~0.01 and 0.15 Hz (Fox and Raichle, 2007). Assumed to have a relatively featureless 1/f-type spectrum, and to be tightly coupled to neuronal activity, these fluctuations are the foundation of so-called 'resting state functional connectivity mapping' (RSFC); an increasingly popular approach to functional magnetic resonance imaging (fMRI). The basis of RSFC mapping is the idea that spatially distinct correlations in the time-course of spontaneous hemodynamic fluctuations (detected as changes in the fMRI blood oxygen level dependent signal, BOLD) can be interpreted as maps of large-scale functional network organization. Such mapping has been demonstrated in mice (White et al., 2011), rats (Pawela et al., 2008), non-human primates (Mantini et al., 2011) and humans (Buckner et al., 2008; Fox and Raichle, 2007) and is increasingly being applied to study the difference between normal and diseased brain states including early Alzheimer's disease (Buckner et al., 2009; Sheline and Raichle, 2013), study of motor deficits in brain tumor patients (Otten et al., 2012), predicting surgical outcome of epilepsy (Negishi et al., 2011), traumatic brain injury (Mayer et al., 2011) and schizophrenia (Garrity et al., 2007).

Distinct from these 1/f-type fluctuations, there have also been reports of a so called ~0.1 Hz, 'vasomotor' or slow sinusoidal hemodynamic oscillation (SSHO) in the brain (Mayhew et al., 1996). These large oscillations, with amplitudes comparable to the hemodynamic response to sensory stimulus, are sporadic, but have been shown to occur in the rat (Golanov et al., 1994; Grosberg et al., 2012; Majeed et al., 2009; Mayhew et al., 1996; Saka et al., 2010), cat (Spitzer et al., 2001), awake rabbit (Hundley et al., 1988) and non-invasively in humans using near-infrared spectroscopy (Elwell et al., 1999; Kolyva et al., 2013;

* Corresponding author.
E-mail address: eh2245@columbia.edu (E.M.C. Hillman).

1053-8119/$ – see front matter © 2013 Elsevier Inc. All rights reserved.
http://dx.doi.org/10.1016/j.neuroimage.2013.10.044

Näsi et al., 2011; Obrig et al., 2000; Sassaroli et al., 2012; Schroeter et al., 2005), and fMRI BOLD (Mitra et al., 1997). In some cases the appearance of SSHOs in the brain has been linked to distinct physiological conditions or states (Näsi et al., 2011). However, a factor that has confused interpretation of these observations is the known occurrence of sinusoidal oscillations in systemic blood pressure, also at around 0.1 Hz, in this case being called 'Mayer waves' (Julien, 2006; Mayer, 1876). The possible influence of systemic blood pressure oscillations on measurements of cortical hemodynamics, particularly non-invasive NIRS measurements through the intact scalp, (Kvernmo et al., 1998) has made the true prevalence, cause, mechanisms and neural correlates of SSHOs unclear.

In this study we present the direct observation of a ~0.1 Hz, spatially distinct cortical hemodynamic oscillation in an awake human undergoing brain tumor resection, acquired using intraoperative multi-spectral optical intrinsic signal imaging (MS-OISI). Intraoperative imaging data collected on a second subject, who was undergoing epilepsy surgery and did not exhibit SSHOs, is shown for comparison. We characterize the spatiotemporal properties of the SSHOs observed in subject 1, identifying correlated oscillations in the tone of pial arterioles, and demonstrating that the SSHOs exhibit wave-like properties within affected regions of the cortex. We further show that a similar ~0.1 Hz oscillation was detected in fMRI BOLD data acquired in the same subject, four days prior to surgery.

We conclude that although only observed here in one subject, SSHOs can occur in the human, awake brain and are measurable via fMRI. We discuss the possible mechanistic underpinnings of SSHOs and their potential importance for diagnostics and RSFC mapping.

Methods

Multi-spectral optical intrinsic signal imaging (MS-OISI)

This study utilized MS-OISI, a technique which uses a camera to acquire images while the cortical surface is illuminated with specific wavelengths of light. Changes in measured light intensity correspond to changes in absorption due to changes in the concentrations of oxy- and deoxy-hemoglobin ([HbO] and [HbR] respectively) (Bouchard et al., 2009; Hillman, 2007). MS-OISI images represent a 2D, superficially weighted sum of these hemodynamic signals from the pial vasculature and the deeper microvasculature of the parenchyma, and can also be used to calculate dynamic changes in vascular tone (Tian et al., 2011). Since the first human intraoperative OISI study (Haglund et al., 1992) researchers have primarily focused on human intraoperative mapping of eloquent cortex (Prakash et al., 2009; Suh et al., 2010), perfusion assessment (Hecht et al., 2013), and neurovascular coupling changes in epileptogenic cortex (Haglund and Hochman, 2004; Zhao et al., 2007). One distinction of our method relative to earlier human work was our choice not to utilize glass to immobilize the cortex. All of our recordings were made quickly and simply via a standard Leica M720 surgical microscope without compromising the sterile surgical field. Brain motion was overcome by using highly uniform illumination and post-hoc image registration as described further below.

Optical data acquisition

All human subject procedures were reviewed and approved by the Columbia University Institutional Review Board. In both patients, a craniotomy was performed to expose the brain under propofol anesthesia. The region of brain exposed was determined by the patient's medical condition, but in both cases was centered on the posterior frontal lobe.

Human subject 1

Images were acquired using sequentially strobed, filtered blue, green, and red light emitting diodes (LEDs, 470, 530, and 625 nm, respectively: M470L2, M530L2, and M625L2; Thorlabs, filters: NT67-027 (blue), NT67-031 (green), Edmund Optics). Strobed illumination was synchronized with high-speed monochrome camera acquisition (AVT Pike F-032B) mounted onto the surgical microscope (Leica M720). Data was recorded using our open-source SPLASSH optical imaging software (Sun et al., 2010), and was collected at 20 frames per second (fps) equivalent to 6.67 fps per wavelength with 480 × 640 pixel resolution over a ~3 × 3 cm field of view.

Human subject 2

Images were acquired using a color camera (Ikegami MKC 505) mounted on the surgical microscope (Leica M720). White light illumination was provided by the microscope's built in xenon arc-lamp (400 W). To gain spectral isolation for blue, green and red channels, we placed a triple-bandpass filter (Semrock FF01-457/530/628-25) before the camera. Filter cutoff properties were chosen to match the spectral response of the camera. Color data was recorded using the microscope's acquisition software (Med X Digital Recording System V6) and was collected at 30 fps per wavelength with a 480 × 640 pixel resolution over a ~3 × 3 cm field of view. This system corresponded to a later, improved version of our first intrasurgical MS-OISI set-up, but has been independently tested to ensure that it yields equivalent data to the system used for subject 1.

Optical data analysis

Post-operatively, 'elastix' image registration software (Klein et al., 2010) was used to correct MS-OISI data for motion artifacts due to the patient's head movement, brain motion caused by heart rate and respiration, and slight microscope motion. Elastix was used to apply non-rigid, bspline-based registration, or where appropriate, rigid registration transformations with supervision to ensure that registration-related errors were not introduced into the data. All subsequent analysis and visualization was performed using Matlab ™. Monotonic trends resulting from evaporation of moisture from the cortical surface (Lavine et al., 2011), were removed from the raw data prior to conversion into ΔHbO and ΔHbR as detailed below. Correlation images were generated by using *corr*, Fourier maps show the log of the time-course power spectrum calculated using *pwelch*, and plotted 'power spectra' are shown as the absolute values of the Fourier transform using *abs* and *fft* Matlab functions (R2012a).

All optical imaging data was converted to ΔHbO and ΔHbR and ΔHbT = ΔHbO + ΔHbR by using the modified Beer–Lambert law with wavelength-dependent path-length factors derived from Monte Carlo modeling (Bouchard et al., 2009; Hillman, 2007). Hemoglobin extinction coefficients were calculated for each system's measured blue, green and red spectral bandwidths based on data collated by Prahl (1998).

fMRI data acquisition

fMRI data was acquired on subject 1, four days prior to surgery, using a 3.0 T magnetic resonance scanner (GE Healthcare Signa HDxt with 8 channel HD Brain Coil). Head movement was restricted using a pillow and foam, and earplugs were used to attenuate scanner noise and maximize subject comfort. During functional imaging, the subject was instructed to close her eyes, but to stay awake and remain as still as possible while performing a left hand motor task during acquisition consisting of a 20 second hand grasp followed by 20 seconds of rest. Data consisted of a total of 80 multi-slice T_2^*-weighted volumes acquired with a gradient echo-planar sequence using axial slice orientation (39 slices, slice thickness = 5 mm, spacing = 0 mm, field of view = 21 cm^2, phase field of view 1.00 cm^2, frequency = 64 Hz, phase = 64, repetition time = 2000 ms, echo time = 30 ms, flip angle = 90°). A T_1 magnetization prepared rapid gradient echo

sequence was also acquired in the same session for co-registration with functional data.

fMRI data analysis

Acquired T_2^* data was pre-processed using FEAT (fMRI Expert Analysis Tool, version 6.00, part of FSL) (Jenkinson et al., 2002) with processing limited to time-interpolation between slices and motion correction. Co-registration between functional and anatomical data was performed manually to avoid registration confounds due to low T_1 contrast in the tumor region. Power spectra are shown as the absolute values of the Fourier transform of extracted T_2^* signals.

Results

Direct observation of ~0.1 Hz oscillation in the awake human cortex

Subject 1 was a 35 year old female undergoing a repeat craniotomy for resection of a right posterior medial frontal lobe oligodendroglioma. During intrasurgical optical imaging, the subject was awake and engaged in performing a hand motor task by pushing a button for the duration of an auditory cue (3 s on, 3 s off). Although the subject was performing a task during MS-OISI acquisition, intrasurgical somatosensory evoked potential monitoring via a strip electrode and pre-operative fMRI data (Fig. 4) confirmed that the receptive field for this task was not within the surgical field of view (see Fig. 4).

The subject was imaged three times over the course of the MS-OISI imaging session. The optical imaging field of view is shown in Fig. 1A. Fig. 1B shows time courses of changes in HbO, HbR and HbT extracted from the 4 regions of interest (ROIs) shown in Fig. 1A for one run (data for the other two runs are shown in Supplemental Figs. S1 and S2). A distinct 0.1 Hz, sinusoidal oscillation in ΔHbO, ΔHbR and ΔHbT is observed in two of these four ROIs, with the strongest oscillation towards the bottom right of the field of view. The power spectra of the ΔHbT time-courses show a prominent peak at ~0.1 Hz (Figs. 2C–D). Additional peaks in the power spectrum correspond to the patient's heart rate (~2.0 Hz) and respiration (~0.4 Hz) frequencies, as confirmed by anesthesia physiological monitoring.

Fig. 1E shows a 'Fourier image', produced by calculating the spectral power of the time-course of each pixel at a given frequency, in this case: 0.1 Hz (Kiviniemi et al., 2000). The resulting image reveals 3 distinct oscillating regions, highlighted with white dashed ovals in Fig. 1E. A Fourier image away from the 0.1 Hz peak, at 0.15 Hz (Fig. 1F), shows no discernible regions, and confirms that regional localization is specific to the 0.1 Hz SSHO.

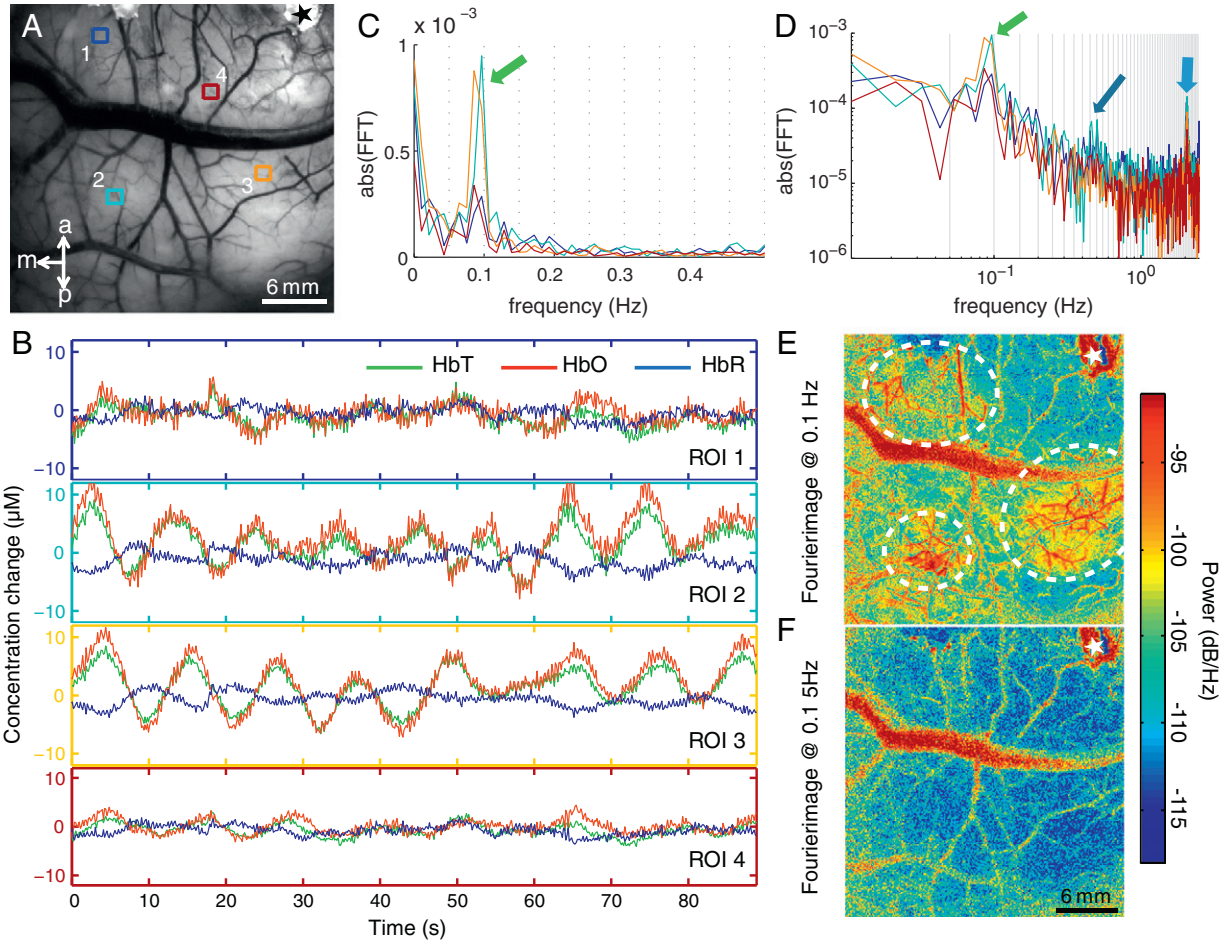

Fig. 1. Direct observation of the 0.1 Hz hemodynamic oscillations in the awake human brain. (A) Grayscale image of subject 1 craniotomy under 530 nm illumination with 4 regions of interest (ROIs) indicated. (B) 4 corresponding time courses showing ΔHbT, ΔHbO and ΔHbR dynamics for each ROI indicated in A. (C) Power spectrum (abs(FFT)) of ΔHbT time courses shown in B. Green arrow indicates SSHO at ~0.1 Hz. (D) Log–log abs(FFT) plot over a wider frequency range showing otherwise 1/f shape. Heart-rate (2 Hz) is indicated by the thick blue arrow, breathing (0.4 Hz) with a thin blue arrow and the SSHO with a green arrow. (E) Fourier image of the field of view at 0.1 Hz, delineating 3 distinct vascular networks, outlined with white dashed ovals (stars indicate artifacts from specular reflections). (F) Fourier image at 0.15 Hz, away from the 0.1 Hz peak in the power spectrum, showing no delineated regions. Supplemental Movie M1 shows the full time-course of the ΔHbT image for the data shown here. Equivalent data for two more runs is shown in Supplemental Figs. S1 and S2.

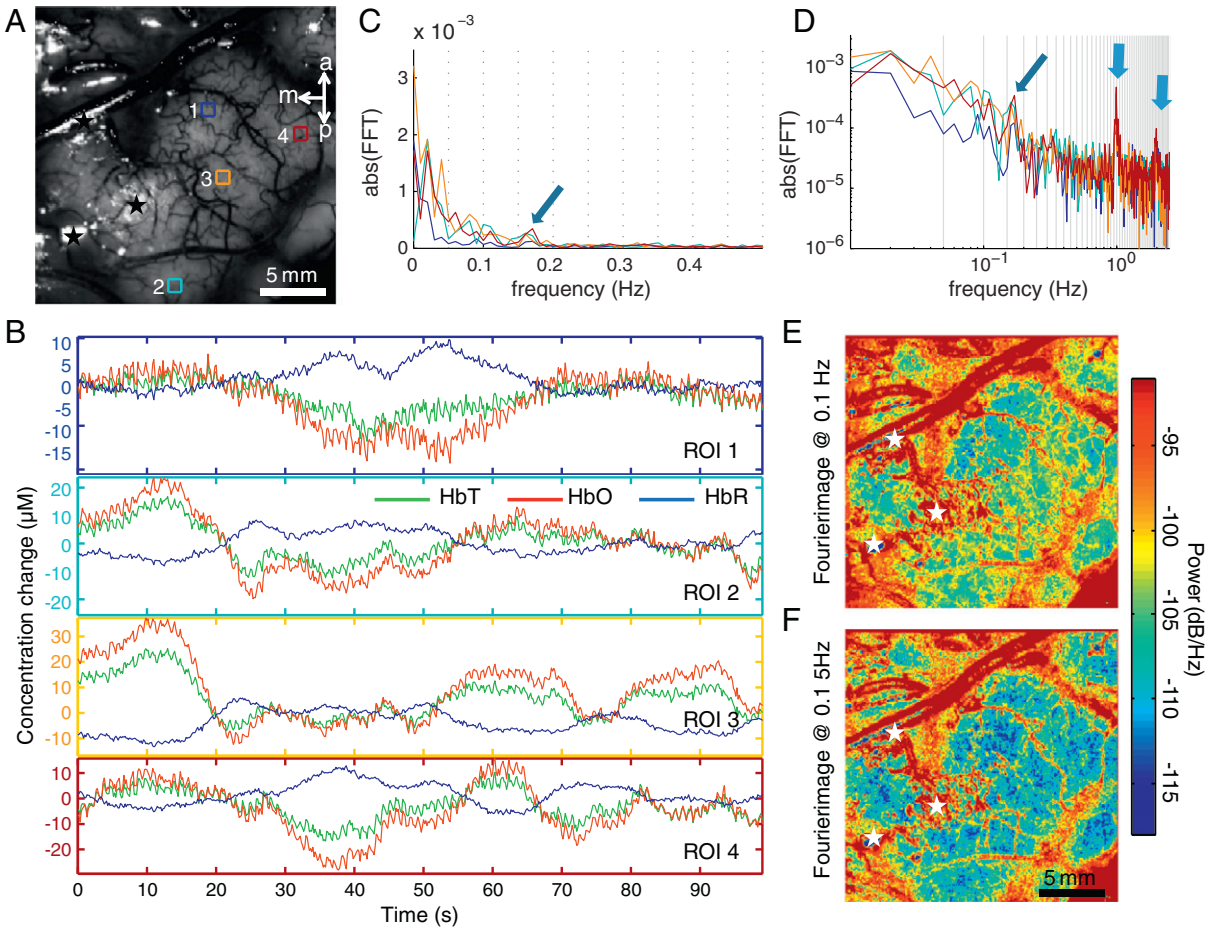

Fig. 2. Non-sinusoidal low frequency hemodynamics in a second human subject. (A) Grayscale image of subject 2 craniotomy under 530 nm illumination with 4 ROIs indicated. (B) 4 corresponding time courses showing ΔHbT, ΔHbO and ΔHbR dynamics for each ROI indicated in A. (C) Power spectrum (abs(FFT)) of HbT time courses shown in B with 0.17 Hz breathing rate indicated by a thin blue arrow. (D) Log–log abs(FFT) plot of wider frequency range with thicker blue arrows indicating heart rate (1 Hz) and its harmonic (2 Hz). (E) Fourier image of the field of view at 0.1 Hz, and (F) a Fourier image at 0.15 Hz. Stars indicate artifacts from specular reflections. No distinct vascular networks are apparent in either image. A movie of ΔHbT dynamics in subject 2 is shown in Supplemental Movie M2.

Non-sinusoidal hemodynamic fluctuations in human cortex (subject 2)

Subject 2 was a 36 year old male undergoing electrode grid placement surgery to locate epileptic foci in the right posterior frontal lobe. The patient was sedated with propofol anesthesia during imaging and no seizure activity was noted during optical recordings. Fig. 2B shows time-courses of ΔHbR, ΔHbO and ΔHbT for 4 ROIs, along with their power spectra (Figs. 2C–D). As confirmed by anesthesia records, a heart rate peak at ~1 Hz, and its harmonic at ~2 Hz, along with a respiration related peak at ~0.17 Hz can be seen for all ROIs, but no 0.1 Hz or similar peak is present. Time courses are markedly different form the time courses in Fig. 1B for subject 1, showing clear low frequency fluctuations, but without a periodic sinusoidal shape. Figs. 2E–F show Fourier images generated at 0.1 Hz and 0.15 Hz. No defined regions oscillating at ~0.1 Hz are discernible. This data confirms that the 0.1 Hz oscillation observed in subject 1 was not a function of an exposed-cortex craniotomy, optical imaging or analysis techniques.

Spatiotemporal and vascular properties of the 0.1 Hz hemodynamic oscillation

Intraoperative MS-OISI provides the opportunity to closely examine the features of the 0.1 Hz hemodynamic oscillation in the human brain. To ascertain the spatial properties of the oscillation observed in subject 1, a Pearson correlation coefficient image was generated (Fig. 3A) by correlating the ΔHbT time course seen in ROI 3 in Fig. 1B with the time course of each pixel in the ΔHbT image time-series. This time course was chosen because of its highest spectral power at 0.1 Hz. The resulting correlation image (Fig. 3A) reveals the distinct spatial localization and extent of the seeded 0.1 Hz oscillation. Note that the relative phase of the oscillation in this region causes it to be isolated from the other SSHO regions identified in the Fourier image Fig. 1E. Magnifying the area with the highest correlation reveals fine vascular structure shown in Fig. 3B. Notably, small vessels under the large central vein are seen to be a continuous part of the ~0.1 Hz oscillating vascular network (arrows in Figs. 3B, C).

To explore these vessels further, we analyzed whether the correlated fluctuations in ΔHbT corresponded to variations in vessel diameter. Vessel diameter calculations were carried out on the raw 530 nm reflectance data, registered using the rigid instead of the non-rigid transformations to avoid vessel motion removal caused by non-rigid registration. Time courses of the changes in HbT and vessel diameter are plotted in Fig. 3D, and show a close correlation of 0.83 between the two signals. We conclude that these vessels are pial arterioles undergoing rhythmic vasomotor dilation and constriction (Grosberg et al., 2012).

Further exploring the observed SSHOs, upon inspection of movies of ΔHbT, distinct epochs were noted in which the 0.1 Hz oscillation appeared to propagate across the cortex as a spatial wave (see Supplemental Movie M1, Supplemental Figs. S1–S2). This wave behavior is visible in the kymograph in Fig. 3E, which shows the detected ΔHbT signal along a line within the field of view as a function

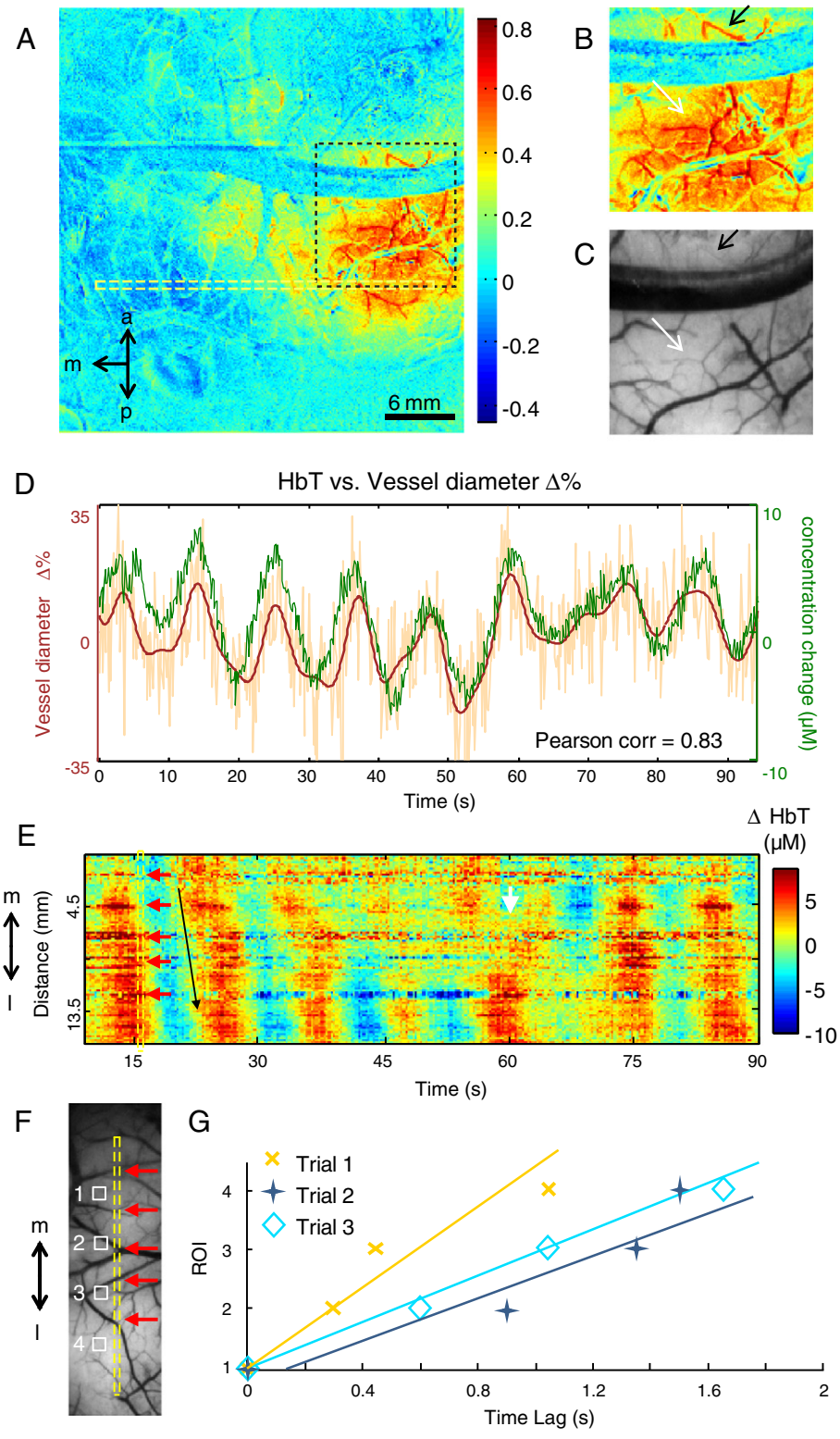

Fig. 3. Properties of the ~0.1 Hz oscillation in the human brain. (A) Pearson correlation coefficient image using the ΔHbT time course from ROI 3 in Fig. 1. (B, C) Magnification and corresponding comparison of the correlation image with raw green channel grayscale image of the region indicated by the black dashed box in A. Note the large vascular network delineated by the correlation image extends under the large vein (black arrow). (D) Change in vessel diameter relating to change in ΔHbT over vessel indicated by white arrow in C. Light brown indicates raw vessel diameter time course, dark brown is the raw vessel diameter time course low pass filtered at 0.2 Hz. (E) Wave-like propagation of the 0.1 Hz oscillation depicted as a ΔHbT kymograph image of time courses extracted along the long dashed yellow ROI in A and in yellow in the inset gray scale image below (F). Red arrows mark pixels corresponding to blood vessels. Black arrow indicates the direction of a single wave's propagation. Equivalent data from two more trials is shown in Supplementary Figs. S1 and S2. White arrow indicates a point of merge. (G) Using cross-correlation analysis, time lags between ~0.1 Hz oscillating time courses extracted from 4 ROIs shown on the grayscale image to the left demonstrate directional propagation of the SSHO wave.

of time. For the first few cycles of the SSHO, the wave can be seen to be propagating in a medial to lateral direction, as is most common across all three runs acquired in this subject (see Supplemental Figs. S1 and S2). However, the kymograph also shows that at certain times, oscillations can travel and merge in different ways. Fig. 3G shows the relative phase delays of SSHOs in four different ROIs during ~50–60 second epochs for all three trials showing clear directional propagation. Phase delays were calculated by cross correlating HbT time courses from ROIs 2,3 and 4 with the HbT time course from ROI 1 and extracting the time value corresponding to the largest correlation in the nearest cycle around 0, for each of the 4 time course pairs.

Pre-operative fMRI in subject 1

fMRI data was acquired on subject 1 four days prior to surgery to assess the location of the left hand motor region in relation to the tumor. The patient performed a similar left hand motor task during fMRI acquisition as during intrasurgical imaging, although at a slower repetition frequency (20 s on, 20 s off).

The approximate location of the optical imaging field of view, as indicated in Fig. 4B, was determined from examination of anatomical T_1 and T_2^* MRI scans and intraoperative MR registration using the BrainLAB® system (Brainlab, Inc. Westchester, IL). Regions responding to the motor task were confirmed to be outside of the intrasurgical imaging field of view by awake intraoperative somatosensory evoked potential mapping using a cortical strip electrode placed along the posterior edge of the cranial window. Examination of the anatomical MRI scan shows that the anterior edge of our optical imaging field of view is located over superficial tumor, but that the posterior side (where most prominent SSHOs were observed) may have some residual cortex overlaying the tumor. Related orthogonal views of the subject's T_1 anatomical scan are shown in Figs. 4K–J.

fMRI BOLD data was minimally pre-processed, as described in the Methods section, and then examined using Fourier analysis and manual inspection of voxel time-courses to identify the ROIs and corresponding time-courses shown in Figs. 4D, E and F. ROI 1 shows the primary right motor cortical region for the left hand, where well-correlated responses to the stimulus were seen (Fig. 4D). Both T_1 and T_2^* signals within the tumor were low, which combined with large voxels made it difficult

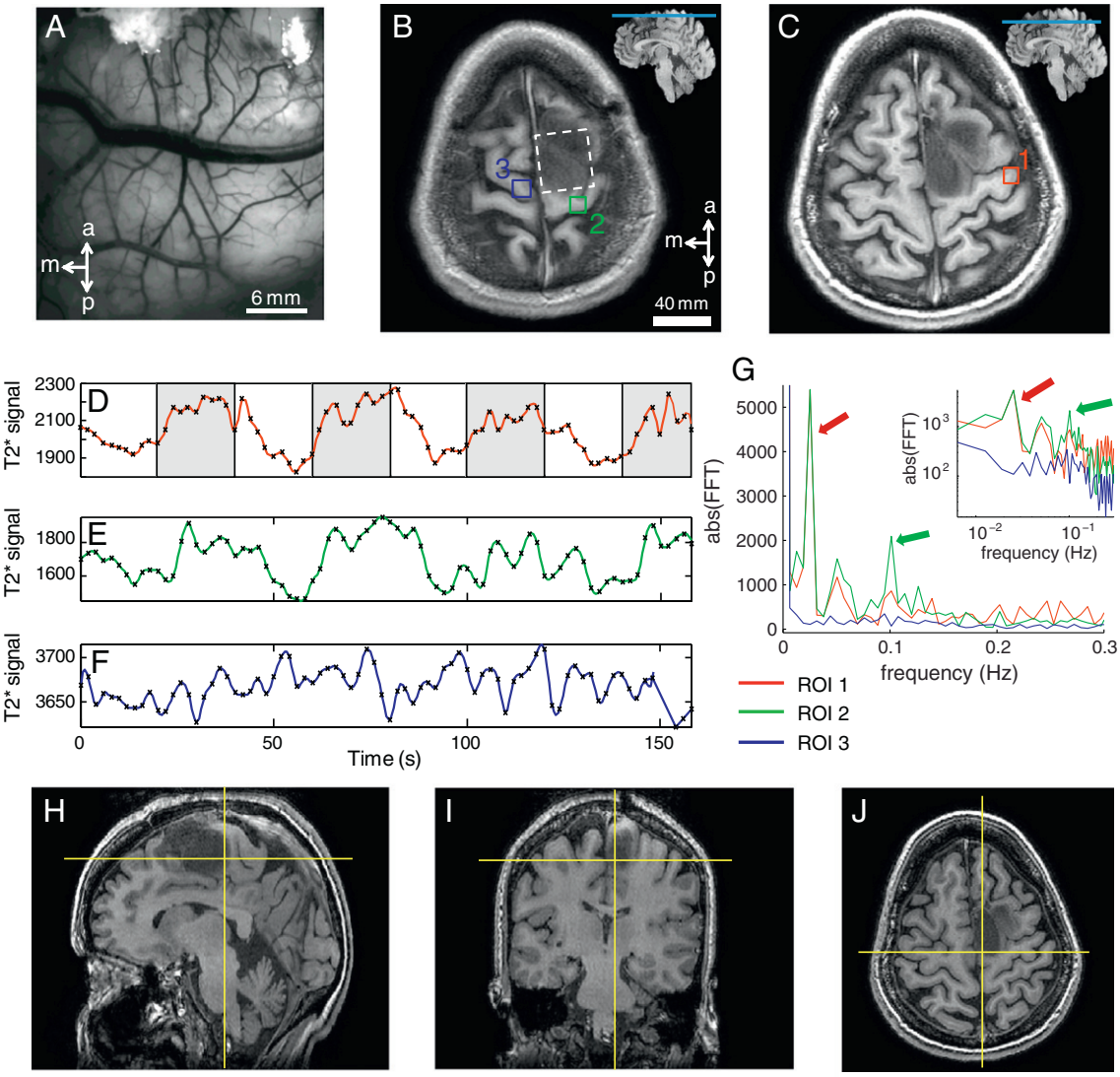

Fig. 4. Observation of 0.1 Hz oscillation in pre-operative fMRI BOLD signal in subject 1. (A) Optical field of view and (B) correspondingly oriented field of view on the MRI outlined by a white dashed region showing 2 ROIs. (C) Additional deeper horizontal section showing an ROI over the left hand region in the right motor cortex. Sagittal view showing the location of the horizontal sections is displayed on the top right for B and C. A = anterior, P = posterior, R = right. (D) BOLD signal responses to left hand task in ROI 1. (E, F) BOLD signal time course from ROI 2 and ROI 3. Black crosses mark measured BOLD time-points. A spline interpolated trace is also shown in each case. (G) Power spectra (abs(FFT)) showing a ~0.1 Hz peak in ROI 2 (indicated by the green arrow). Peak frequency corresponding to the left hand task is indicated by the brown arrow. (inset) Power spectra (abs(FFT)) from (G) plotted on a log–log scale, showing 1/f behavior. (H, I, J) Saggital, coronal and horizontal views of subject 1 respectively, showing the location and extent of the tumor.

to extract time-courses from the uppermost surface of the tumor/cortex corresponding to the exact area of our intraoperative recordings. However, ROI 2 was selected from the superior edge of the left hand motor area, at the posterior edge of our optical imaging field of view, and in addition to exhibiting a small stimulus response exhibits very similar 0.1 Hz BOLD oscillations to those observed intraoperatively (Fig. 4E, power spectrum 4G). ROI 3 is a region from the cortex contralateral to the tumor, and while exhibiting slow fluctuations in BOLD (Fig. 4F) can be seen to have a featureless 1/f spectrum with no peak at 0.1 Hz (Fig. 4G).

Discussion

Slow sinusoidal 0.1 Hz hemodynamic oscillations, or SSHOs in humans have been reported previously using both NIRS and fMRI BOLD (Mitra et al., 1997; Obrig et al., 2000). However, the prevalence and importance of SSHOs have been questioned, particularly in relation to contamination from systemic blood pressure fluctuations (Ferguson, 2003; Kvernmo et al., 1998). Using intraoperative MS-OISI we recorded optical reflectance signals directly from the superficial layers of the awake human cortex, unobstructed by confounds from the scalp and skull. The substantially higher spatiotemporal resolution of MS-OISI compared to NIRS and fMRI measurements allowed analysis of time courses of ΔHbO, ΔHbR, ΔHbT and vasomotion dynamics, demonstrating that observed SSHOs were associated with distinct networks of pial arterioles. Visualization of SSHOs propagating as a traveling wave within discrete regions of the cortex suggests that the oscillation is not a manifestation of systemic blood pressure 'Mayer waves'. fMRI data acquired in the same patient prior to surgery revealed that similar ~0.1 Hz SSHOs could be observed as fluctuations in the raw BOLD signal.

Since our data demonstrates that localized 0.1 Hz oscillations in cortical hemodynamics can occur in the awake human brain, and that these oscillations can be detected by fMRI, the physiological basis of these oscillations, and how to interpret them, becomes a key question. Of particular importance is whether 0.1 Hz hemodynamic oscillations in the brain are neurogenic; driven by a specific neuronal state or sequence of activity, or whether oscillations are myogenic; driven by the vasculature itself independent of neuronal activity. We propose that our findings, combined with the evidence detailed below, suggest that 0.1 Hz oscillations are primarily myogenic.

Prior studies suggest neurovascular uncoupling during SSHOs

Despite numerous reports of SSHOs in animal models, the physiological basis of SSHOs in the brain has barely been explored. While several recent studies have found electrophysiological correlates to slow hemodynamic fluctuations in fMRI BOLD at <0.1 Hz (Drew et al., 2008; Leopold et al., 2003; Lőrincz et al., 2009; Nir et al., 2008), only a small number of studies have specifically noted the relationship between neuronal activity and the ~0.1 Hz hemodynamic oscillation. One recent study using combined spectrophotometry and electrophysiology to study neurovascular coupling in the visual thalamus of a cat, and reported spontaneous SSHOs at 0.14 Hz, which were inducible by chloralose anesthesia and could be temporarily blocked by systemic administration of adrenaline or acetylcholine (Rivadulla et al., 2011). The authors demonstrated a marked breakdown in the relationship between local neural activity and blood flow when oscillations were present. Another study using laser Doppler to measure blood flow combined with electroencephalography (EEG) in rats during isoflurane-induced neuronal bursting, noted that in instances when 'strong sinusoidal' hemodynamic fluctuations at around 0.1 Hz arose following sharp blood pressure changes, correlations between neuronal and hemodynamic measures were abolished (Golanov et al., 1994).

Is there something special about 0.1 Hz?

It is well known that isolated blood vessels, from the brain and peripheral vasculature across species can exhibit spontaneous rhythmic 'vasomotor' oscillations in tone in the frequency range of 0.05–0.2 Hz (Aalkjær et al., 2011; Aalkjær and Nilsson, 2005; Fujii et al., 1990; Oishi et al., 2002; Peng et al., 2001; Stefanovska, 2007). In the past 10 years, this phenomenon has been studied in detail (Aalkjær et al., 2011), and ~0.1 Hz has been identified as a characteristic frequency for arterioles from diverse locations and species (Bouskela and Grampp, 1992; Haddock et al., 2002; Setchell et al., 1995). In isolated vessels, vasomotion at ~0.1 Hz has been shown to correspond to synchronization of the intermittent release of calcium within vascular smooth muscle cells (Aalkjær et al., 2011). While the mechanisms initiating this synchronization, and the cyclic process that sustains the oscillation are not well understood (Aalkjær and Nilsson, 2005; Haddock and Hill, 2005; Kapela et al., 2012), a range of different factors have been shown to lead to this synchronous state. These include conditions where microcirculation is at the lower end of the systemic autoregulatory pressure range (Ren et al., 1994; Schmidt et al., 1992), peripheral arterial occlusion disease (Schmidt et al., 1993), and in patients after compression therapy (Pekanmäki et al., 1991). The amplitude and frequency of vasomotion has been shown to be temperature dependent (Setchell et al., 1995), and affected by local changes in PO_2 and pH (Bouskela and Grampp, 1992). Most reports of vasomotion in peripheral vessels conclude that it is myogenic in origin, driven by the properties of the vessels themselves in response to external conditions (Bouskela and Grampp, 1992).

Are all brain SSHOs the same?

SSHOs have been observed in the brain in a wide range of conditions. Some have dismissed SSHOs as a consequence of anesthesia, abnormal blood pressure, sudden blood pressure changes, or an artifact of non-physiological open cortex surgical conditions (Golanov et al., 1994; Jones et al., 2005; Julien, 2006; Nakai and Maeda, 1999). Nitric oxide (NO) blockers and ketamine anesthesia have also been noted to induce marked enhancement of SSHOs in animal models (Ances et al., 2010; Dirnagl et al., 1993; Spitzer et al., 2001). Further studies have reported anomalous, low frequency periodic oscillations in brain blood flow in a range of pathological conditions including neuroleukemia, hydrocephalus and glioma (Kiviniemi et al., 2000; Wang et al., 2008). However, SSHOs have also been observed non-invasively in healthy awake humans using both NIRS and fMRI (Elwell et al., 1999; Mitra et al., 1997; Obrig et al., 2000).

The distinctive frequency of SSHOs suggest that each of these diverse conditions shares some common property. Based on the considerations above, we hypothesize that SSHOs might be an outward indication that some factor of normal hemodynamic regulation in the brain has been altered, whether by a transient physiological or attentional state, a pharmacological agent or a local or global pathology. We posit that 0.1 Hz may be a uniquely important frequency, noting that the time-constant of its cycle is highly consistent with the functional 'hemodynamic response function', which typically peaks 3–4 s after the onset of a stimulus (Kruggel and von Cramon, 1999); suggesting that 0.1 Hz might be the brain's hemodynamic natural frequency. Observations of SSHOs in the brain during periods of low blood pressure or flow, or sudden changes in blood pressure would be consistent with observations of vasomotion in the peripheral vasculature (Sakurai and Terui, 2006; Schmidt et al., 1992). NO inhibitors and ketamine could both be expected to induce an imbalance in the normal regulation of cerebrovascular tone (Anis et al., 1983; Attwell et al., 2010; Harrison and Simmonds, 1985). In the case of pathologies; situations in which any component of the neurovascular unit or autoregulatory system including endothelial cells, smooth muscle cells, astrocytes or neurons themselves might be damaged or impaired could potentially result in

SSHOs. For example, glioma cells have been shown to spread via migration along the vasculature (Farin et al, 2006), a disruptive action that could easily interfere with the local vasculature's ability to maintain normal tone. We note that the patient in whom we observed SSHOs was undergoing resection of a recurrent oligodendroglioma. Both the cellular presence of the tumor, and perfusion deficits caused by compression or stretching of overlying cortex (depicted in Figs. 4H–J) could potentially account for the presence of SSHOs.

While requiring further investigation, we infer that the appearance of SSHOs might represent a departure from normal neurovascular coupling.

Implications for interpretation of functional imaging studies and functional diagnostics

From the first demonstration of functional connectivity MRI (fcMRI) in the human sensorimotor cortex (Biswal et al., 1995), RSFC algorithms have commonly applied a low-pass cutoff filter at ~0.08 Hz (Fox et al., 2005) with the intent of removing artifacts from human breathing frequencies. However, the proximity of this cut-off to 0.1 Hz makes it possible that SSHOs, if present, could have a major influence on RSFC related analysis. To date, the presence of this oscillation in resting state fMRI has rarely been noted or specifically analyzed, so its prevalence and relevance to RSFC results in different pathologies have not been explored (Murphy et al., 2013; Wang et al., 2008). fcMRI is increasingly being applied to pathological states including acute and chronic stroke (Grefkes and Fink, 2011), Alzheimer's disease (Sheline and Raichle, 2013), and traumatic brain injury (Mayer et al., 2011); all conditions in which SSHOs could feasibly arise, and all conditions in which alterations in resting state networks have been demonstrated.

While SSHOs could potentially confound conventional interpretation of resting state fMRI data, our findings present the exciting opportunity that SSHOs themselves could be markers of neurovascular abnormalities, and thus early markers of disease or prognosis. Our observation of SSHOs in a patient with a recurrent oligodendroglioma both presurgically via fMRI and then intraoperatively using MS-OISI suggests that SSHOs could provide important new, previously unexplored biomarkers, detectable non-invasively via conventional fMRI BOLD techniques (Wang et al., 2008).

Since BOLD is primarily sensitive to HbR, it is important to note that in our optical recordings, HbR represented a smaller contribution than changes in HbT (Fig. 1B), likely due to the strong arteriolar contribution to SSHOs (Fig. 2B). We also note that identifying regions exhibiting 0.1 Hz oscillations in fMRI data acquired at 0.5 Hz required careful examination of the data's power spectra since at low sample rates, it can be challenging to distinguish a sinusoidal 0.1 Hz wave from both normal baseline fluctuations and aliasing. Nevertheless, regions exhibiting a distinct 0.1 Hz wave were clearly detected in our data, in some cases prominently, confirming that it is possible to detect SSHOs using fMRI.

Supplementary data to this article can be found online at http://dx.doi.org/10.1016/j.neuroimage.2013.10.044.

Acknowledgments

We thank Drs. Catherine Schevon, Angela Lignelli-Dipple, Jack Grinband, Sameer Sheth, John Sheehy, Hani Malone, Daniel Stoyanov, Daniel Chow, Mariel Kozberg and Jason Berwick for helpful discussions; Drs. Michael Sisti and Jeffrey Bruce, Columbia University neurosurgery residents, and neurosurgical operating room staff for their help in collecting the data; Keith Yeager for machining assistance; and members of the Laboratory for Functional Optical Imaging for their support and helpful discussions. We acknowledge support from National Institutes of Health: UL1 RR024156, National Center for Advancing Translational Sciences, Irving Institute CTSA, National Institute of Neurological Disorders and Stroke, 1R01NS063226, 1R01NS076628, and R21NS053684 (to E.M.C.H.); National Science Foundation Grants CAREER 0954796 (to E.M.C.H.); Graduate Fellowship (M.B.B.); National Defense Science and Engineering Graduate Fellowship (to M.B.B.), Doris Duke Foundation research fellowship (T.J.W.); the Human Frontier Science Program and the Kavli Foundation.

References

Aalkjær, C., Nilsson, H., 2005. Vasomotion: cellular background for the oscillator and for the synchronization of smooth muscle cells. Br. J. Pharmacol. 144, 605–616.
Aalkjær, C., Boedtkjer, D., Matchkov, V., 2011. Vasomotion — what is currently thought? Acta Physiol. 202, 253–269.
Ances, B.M., Greenberg, J.H., Detre, J.A., 2010. Interaction between nitric oxide synthase inhibitor induced oscillations and the activation flow coupling response. Brain Res. 1309, 19–28.
Anis, N.A., Berry, S.C., Burton, N.R., Lodge, D., 1983. The dissociative anaesthetics, ketamine and phencyclidine, selectively reduce excitation of central mammalian neurones by N-methyl-aspartate. Br. J. Pharmacol. 79, 565–575.
Attwell, D., Buchan, A.M., Charpak, S., Lauritzen, M., MacVicar, B.A., Newman, E.A., 2010. Glial and neuronal control of brain blood flow. Nature 468, 232–243.
Biswal, B., Yetkin, F.Z., Haughton, V.M., Hyde, J.S., 1995. Functional connectivity in the motor cortex of resting human brain using echo-planar MRI. Magn. Reson. Med. 34, 537–541.
Bouchard, M.B., Chen, B.R., Burgess, S.A., Hillman, E.M.C., 2009. Ultra-fast multispectral optical imaging of cortical oxygenation, blood flow, and intracellular calcium dynamics. Opt. Express 17, 15670–15678.
Bouskela, E., Grampp, W., 1992. Spontaneous vasomotion in hamster cheek pouch arterioles in varying experimental conditions. Am. J. Physiol. Heart Circ. Physiol. 262, H478–H485.
Buckner, R.L., Andrews-Hanna, J.R., Schacter, D.L., 2008. The brain's default network. Ann. N. Y. Acad. Sci. 1124, 1–38.
Buckner, R.L., Sepulcre, J., Talukdar, T., Krienen, F.M., Liu, H., Hedden, T., Andrews-Hanna, J.R., Sperling, R.A., Johnson, K.A., 2009. Cortical hubs revealed by intrinsic functional connectivity: mapping, assessment of stability, and relation to Alzheimer's disease. J. Neurosci. 29, 1860–1873.
Dirnagl, U., Lindauer, U., Villringer, A., 1993. Nitric oxide synthase blockade enhances vasomotion in the cerebral microcirculation of anesthetized rats. Microvasc. Res. 45, 318–323.
Drew, P.J., Duyn, J.H., Golanov, E., Kleinfeld, D., 2008. Finding coherence in spontaneous oscillations. Nat. Neurosci. 11, 991–993.
Elwell, C.E., Springett, R., Hillman, E., Delpy, D.T., 1999. Oscillations in cerebral haemodynamics. Implications for functional activation studies. Adv. Exp. Med. Biol. 471, 57–65.
Farin, A., Suzuki, S.O., Weiker, M., Goldman, J.E., Bruce, J.N., Canoll, P., 2006. Transplanted glioma cells migrate and proliferate on host brain vasculature: a dynamic analysis. Glia 53, 799–808.
Ferguson, A., 2003. A review of the physiology of cranial osteopathy. J. Osteopath. Med. 6, 74–84.
Fox, M.D., Raichle, M.E., 2007. Spontaneous fluctuations in brain activity observed with functional magnetic resonance imaging. Nat. Rev. Neurosci. 8, 700–711.
Fox, M.D., Snyder, A.Z., Vincent, J.L., Corbetta, M., Van Essen, D.C., Raichle, M.E., 2005. The human brain is intrinsically organized into dynamic, anticorrelated functional networks. Proc. Natl. Acad. Sci. U. S. A. 102, 9673–9678.
Fujii, K., Heistad, D.D., Faraci, F.M., 1990. Vasomotion of basilar arteries in vivo. Am. J. Physiol. Heart Circ. Physiol. 258, H1829–H1834.
Garrity, A.G., Pearlson, G.D., McKiernan, K., Lloyd, D., Kiehl, K.A., Calhoun, V.D., 2007. Aberrant "default mode" functional connectivity in schizophrenia. Am. J. Psychiatr. 164, 450–457.
Golanov, E.V., Yamamoto, S., Reis, D.J., 1994. Spontaneous waves of cerebral blood flow associated with a pattern of electrocortical activity. Am. J. Physiol. Regul. Integr. Comp. Physiol. 266, R204–R214.
Grefkes, C., Fink, G.R., 2011. Reorganization of cerebral networks after stroke: new insights from neuroimaging with connectivity approaches. Brain 134, 1264–1276.
Grosberg, L.E., Chen, B.R., Hillman, E.M.C., 2012. Simultaneous multiplane in vivo nonlinear microscopy using spectral encoding. Opt. Lett. 37, 2967–2969.
Haddock, R.E., Hill, C.E., 2005. Rhythmicity in arterial smooth muscle. J. Physiol. 566, 645–656.
Haddock, R.E., Hirst, G.D.S., Hill, C.E., 2002. Voltage independence of vasomotion in isolated irideal arterioles of the rat. J. Physiol. 540, 219–229.
Haglund, M.M., Hochman, D.W., 2004. Optical imaging of epileptiform activity in human neocortex. Epilepsia 45, 43–47.
Haglund, M.M., Ojemann, G.A., Hochman, D.W., 1992. Optical imaging of epileptiform and functional activity in human cerebral cortex. Nature 358, 668–671.
Harrison, N.L., Simmonds, M.A., 1985. Quantitative studies on some antagonists of N-methyl D-aspartate in slices of rat cerebral-cortex. Br. J. Pharmacol. 84, 381–391.
Hecht, N., Woitzik, J., Konig, S., Horn, P., Vajkoczy, P., 2013. Laser speckle imaging allows real-time intraoperative blood flow assessment during neurosurgical procedures. J. Cereb. Blood Flow Metab. 33, 1000–1007.
Hillman, E.M.C., 2007. Optical brain imaging in vivo: techniques and applications from animal to man. J. Biomed. Opt. 12 [051402-051402].
Hundley, W.G., Renaldo, G.J., Levasseur, J.E., Kontos, H.A., 1988. Vasomotion in cerebral microcirculation of awake rabbits. Am. J. Physiol. Heart Circ. Physiol. 254, H67–H71.

Jenkinson, M., Bannister, P., Brady, M., Smith, S., 2002. Improved optimization for the robust and accurate linear registration and motion correction of brain images. NeuroImage 17, 825–841.
Jones, M., Berwick, J., Hewson-Stoate, N., Gias, C., Mayhew, J., 2005. The effect of hypercapnia on the neural and hemodynamic responses to somatosensory stimulation. NeuroImage 27, 609–623.
Julien, C., 2006. The enigma of Mayer waves: facts and models. Cardiovasc. Res. 70, 12–21.
Kapela, A., Parikh, J., Tsoukias, Nikolaos M., 2012. Multiple factors influence calcium synchronization in arterial vasomotion. Biophys. J. 102, 211–220.
Kiviniemi, V., Jauhiainen, J., Tervonen, O., Pääkkö, E., Oikarinen, J., Vainionpää, V., Rantala, H., Biswal, B., 2000. Slow vasomotor fluctuation in fMRI of anesthetized child brain. Magn. Reson. Med. 44, 373–378.
Klein, S., Staring, M., Murphy, K., Viergever, M.A., Pluim, J.P.W., 2010. elastix: a toolbox for intensity-based medical image registration. IEEE Trans. Med. Imaging 29, 196–205.
Kolyva, C., Kingston, H., Tachtsidis, I., Mohanty, S., Mishra, S., Patnaik, R., Maude, R., Dondorp, A., Elwell, C., 2013. Oscillations in cerebral haemodynamics in patients with falciparum malaria. In: Welch, W.J., Palm, F., Bruley, D.F., Harrison, D.K. (Eds.), Oxygen Transport to Tissue XXXIV. Springer, New York, pp. 101–107.
Kruggel, F., von Cramon, D.Y., 1999. Temporal properties of the hemodynamic response in functional MRI. Hum. Brain Mapp. 8, 259–271.
Kvernmo, H.D., Stefanovska, A., Bracic, M., Kirkebøen, K.A., Kvernebo, K., 1998. Spectral analysis of the laser Doppler perfusion signal in human skin before and after exercise. Microvasc. Res. 56, 173–182.
Lavine, M., Haglund, M.M., Hochman, D.W., 2011. Dynamic linear model analysis of optical imaging data acquired from the human neocortex. J. Neurosci. Methods 199, 346–362.
Leopold, D.A., Murayama, Y., Logothetis, N.K., 2003. Very slow activity fluctuations in monkey visual cortex: implications for functional brain imaging. Cereb. Cortex 13, 422–433.
Lőrincz, M.L., Geall, F., Bao, Y., Crunelli, V., Hughes, S.W., 2009. ATP-dependent infra-slow (<0.1 Hz) oscillations in thalamic networks. PLoS ONE 4, e4447.
Majeed, W., Magnuson, M., Keilholz, S.D., 2009. Spatiotemporal dynamics of low frequency fluctuations in BOLD fMRI of the rat. J. Magn. Reson. Imaging 30, 384–393.
Mantini, D., Gerits, A., Nelissen, K., Durand, J.-B., Joly, O., Simone, L., Sawamura, H., Wardak, C., Orban, G.A., Buckner, R.L., Vanduffel, W., 2011. Default mode of brain function in monkeys. J. Neurosci. 31, 12954–12962.
Mayer, S., 1876. Studien zur physiologie des herzens und blutgeflaesse V. Ueber spontane blutdruckschwankungen. Akademie der Wissenschaften in Wien. Math. Naturwiss. Cl. 74, 281–307.
Mayer, A.R., Mannell, M.V., Ling, J., Gasparovic, C., Yeo, R.A., 2011. Functional connectivity in mild traumatic brain injury. Hum. Brain Mapp. 32, 1825–1835.
Mayhew, J.E.W., Askew, S., Zheng, Y., Porrill, J., Westby, G.W.M., Redgrave, P., Rector, D.M., Harper, R.M., 1996. Cerebral vasomotion: a 0.1-Hz oscillation in reflected light imaging of neural activity. NeuroImage 4, 183–193.
Mitra, P.P., Ogawa, S., Hu, X., U urbil, K., 1997. The nature of spatiotemporal changes in cerebral hemodynamics as manifested in functional magnetic resonance imaging. Magn. Reson. Med. 37, 511–518.
Murphy, K., Birn, R.M., Bandettini, P.A., 2013. Resting-state fMRI confounds and cleanup. NeuroImage 80, 349–359.
Nakai, M., Maeda, M., 1999. Scopolamine-sensitive and resistant components of increase in cerebral cortical blood flow elicited by periaqueductal gray matter of rats. Neurosci. Lett. 270, 173–176.
Näsi, T., Virtanen, J., Noponen, T., Toppila, J., Salmi, T., Ilmoniemi, R.J., 2011. Spontaneous hemodynamic oscillations during human sleep and sleep stage transitions characterized with near-infrared spectroscopy. PLoS ONE 6, e25415.
Negishi, M., Martuzzi, R., Novotny, E.J., Spencer, D.D., Constable, R.T., 2011. Functional MRI connectivity as a predictor of the surgical outcome of epilepsy. Epilepsia 52, 1733–1740.
Nir, Y., Mukamel, R., Dinstein, I., Privman, E., Harel, M., Fisch, L., Gelbard-Sagiv, H., Kipervasser, S., Andelman, F., Neufeld, M.Y., Kramer, U., Arieli, A., Fried, I., Malach, R., 2008. Interhemispheric correlations of slow spontaneous neuronal fluctuations revealed in human sensory cortex. Nat. Neurosci. 11, 1100–1108.
Obrig, H., Neufang, M., Wenzel, R., Kohl, M., Steinbrink, J., Einhäupl, K., Villringer, A., 2000. Spontaneous low frequency oscillations of cerebral hemodynamics and metabolism in human adults. NeuroImage 12, 623–639.
Oishi, H., Schuster, A., Lamboley, M., Stergiopulos, N., Meister, J.-J., Bény, J.-L., 2002. Role of membrane potential in vasomotion of isolated pressurized rat arteries. Life Sci. 71, 2239–2248.
Otten, M.L., Mikell, C.B., Youngerman, B.E., Liston, C., Sisti, M.B., Bruce, J.N., Small, S.A., McKhann, G.M., 2012. Motor deficits correlate with resting state motor network connectivity in patients with brain tumours. Brain 135, 1017–1026.
Pawela, C.P., Biswal, B.B., Cho, Y.R., Kao, D.S., Li, R., Jones, S.R., Schulte, M.L., Matloub, H.S., Hudetz, A.G., Hyde, J.S., 2008. Resting-state functional connectivity of the rat brain. Magn. Reson. Med. 59, 1021–1029.
Pekanmäki, K., Kolari, P.J., Kiistala, U., 1991. Laser Doppler vasomotion among patients with post-thrombotic venous insufficiency: effect of intermittent pneumatic compression. VASA 20, 394–397.
Peng, H., Matchkov, V., Ivarsen, A., Aalkjær, C., Nilsson, H., 2001. Hypothesis for the initiation of vasomotion. Circ. Res. 88, 810–815.
Prahl, S.A., 1998. Online resource. http://omlc.ogi.edu/spectra/hemoglobin/summary.html.
Prakash, N., Uhlemann, F., Sheth, S.A., Bookheimer, S., Martin, N., Toga, A.W., 2009. Current trends in intraoperative optical imaging for functional brain mapping and delineation of lesions of language cortex. NeuroImage 47 (Supplement 2), T116–T126.
Ren, T.-Y., Brown, J.N., Nuttall, A.L., Miller, J.M., 1994. Cochlear flux motion and arterial pressure reduction in guinea pig. Acta Otolaryngol. 114, 254–258.
Rivadulla, C., de Labra, C., Grieve, K.L., Cudeiro, J., 2011. Vasomotion and neurovascular coupling in the visual thalamus in vivo. PLoS ONE 6, e28746.
Saka, M., Berwick, J., Jones, M., 2010. Linear superposition of sensory-evoked and ongoing cortical hemodynamics. Front. Neuroenerg. 2.
Sakurai, T., Terui, N., 2006. Effects of sympathetically induced vasomotion on tissue–capillary fluid exchange. Am. J. Physiol. Heart Circ. Physiol. 291, H1761–H1767.
Sassaroli, A., Pierro, M., Bergethon, P.R., Fantini, S., 2012. Low-frequency spontaneous oscillations of cerebral hemodynamics investigated with near-infrared spectroscopy: a review. IEEE J. Sel. Top. Quantum Electron. 18, 1478–1492.
Schmidt, J.A., Intaglietta, M., Borgstrom, P., 1992. Periodic hemodynamics in skeletal muscle during local arterial pressure reduction. J. Appl. Physiol. 73, 1077–1083.
Schmidt, J.A., Borgström, P., Firestone, G.P., von Wichert, P., Intaglietta, M., Fronek, A., 1993. Periodic hemodynamics (flow motion) in peripheral arterial occlusive disease. J. Vasc. Surg. 18, 207–215.
Schroeter, M.L., Bucheler, M.M., Preul, C., Scheid, R., Schmiedel, O., Guthke, T., von Cramon, D.Y., 2005. Spontaneous slow hemodynamic oscillations are impaired in cerebral microangiopathy. J. Cereb. Blood Flow Metab. 25, 1675–1684.
Setchell, B.P., Bergh, A., Widmark, A., Damber, J.E., 1995. Effect of testicular temperature on vasomotion and blood flow. Int. J. Androl. 18, 120–126.
Sheline, Y.I., Raichle, M.E., 2013. Resting state functional connectivity in preclinical Alzheimer's disease. Biol. Psychiatry 74, 340–347.
Spitzer, M.W., Calford, M.B., Clarey, J.C., Pettigrew, J.D., Roe, A.W., 2001. Spontaneous and stimulus-evoked intrinsic optical signals in primary auditory cortex of the cat. J. Neurophysiol. 85, 1283–1298.
Stefanovska, A., 2007. Coupled oscillatros: complex but not complicated cardiovascular and brain interactions. IEEE Eng. Med. Biol. Mag. 26, 25–29.
Suh, M., Ma, H., Zhao, M., Geneslaw, A., Schwartz, T., 2010. Intraoperative optical imaging of human cortex. In: Roe, A.W. (Ed.), Imaging the Brain With Optical Methods. Springer, New York, pp. 135–157.
Sun, R., Bouchard, M.B., Hillman, E.M.C., 2010. SPLASSH: open source software for camera-based high-speed, multispectral in-vivo optical image acquisition. Biomed. Opt. Express 1, 385–397.
Tian, P., Devor, A., Sakadžić, S., Dale, A.M., Boas, D.A., 2011. Monte Carlo simulation of the spatial resolution and depth sensitivity of two-dimensional optical imaging of the brain. J. Biomed. Opt. 16 (016006-016006-016013).
Wang, H.H., Menezes, N.M., Zhu, M.W., Ay, H., Koroshetz, W.J., Aronen, H.J., Karonen, J.O., Liu, Y., Nuutinen, J., Wald, L.L., Sorensen, A.G., 2008. Physiological noise in MR images: an indicator of the tissue response to ischemia? J. Magn. Reson. Imaging 27, 866–871.
White, B.R., Bauer, A.Q., Snyder, A.Z., Schlaggar, B.L., Lee, J.-M., Culver, J.P., 2011. Imaging of functional connectivity in the mouse brain. PLoS ONE 6, e16322.
Zhao, M., Suh, M., Ma, H., Perry, C., Geneslaw, A., Schwartz, T.H., 2007. Focal increases in perfusion and decreases in hemoglobin oxygenation precede seizure onset in spontaneous human epilepsy. Epilepsia 48, 2059–2067.